CONF-9009123--5

UCRL-JC-103797
PREPRINT

Modified-Yee Field Solutions in the AMOS Wakefield Code

C. C. Shang
J. F. DeFord

This paper was prepared for submittal to
the
1990 Linear Accelerator Conference
Albuquerque, New Mexico
September 10-14, 1990

August 29, 1990

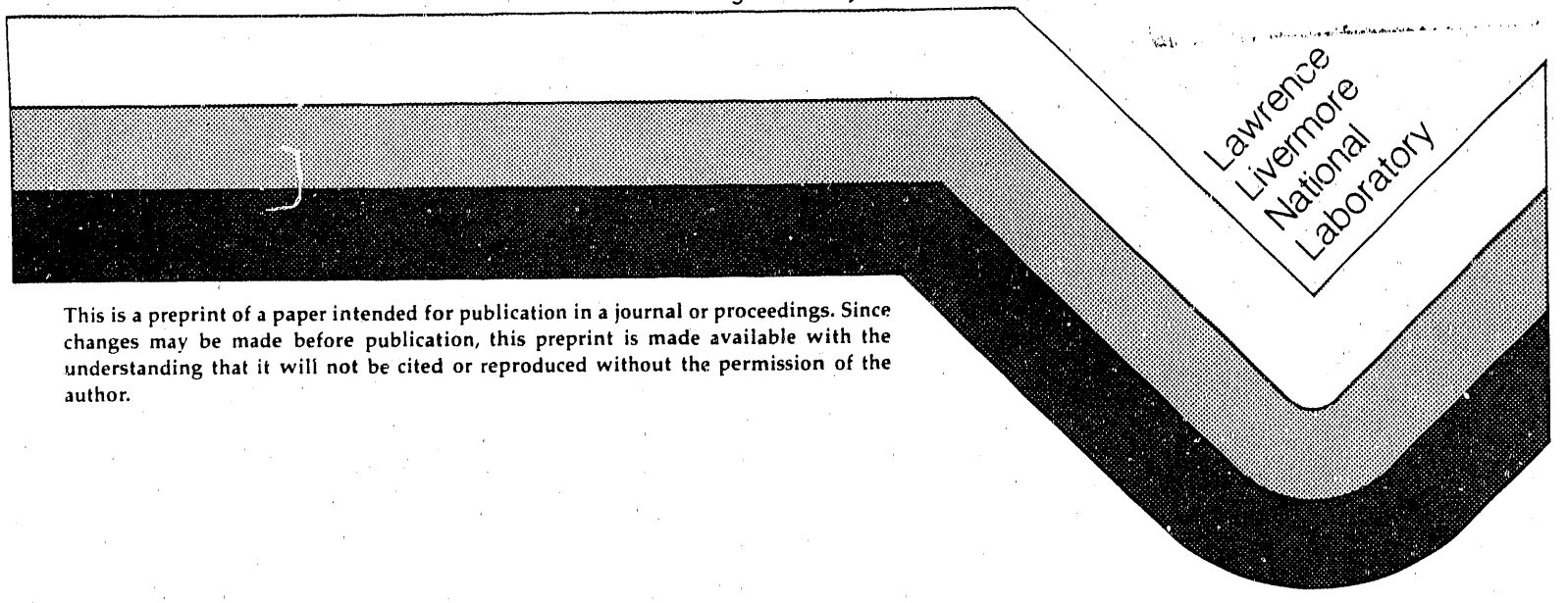

MODIFIED-YEE FIELD SOLUTIONS IN THE AMOS WAKEFIELD CODE *

C. C. Shang and J. F. DeFord
L-626, LLNL, Livermore, CA 94550

UCRL-JC--103797

DE91 000258

Abstract

A new numerical procedure by which field calculations in AMOS [1] are upgraded to model rotationally symmetric cavity structures in a more accurate fashion is described. The development work is aimed at implementing a modified finite difference update scheme on an irregular grid system. Elements of an irregular grid may be chosen to better fit object boundaries, resulting in increased solution accuracy. Our approach involves the placement of field components on a non-orthogonal body fitting grid and on a dual grid which is orthogonal to the first grid. It is found that this procedure retains several important computational advantages, including the ability to exploit the implied spatial relationships between nodes. Propagating fields on an irregular grid system have been observed and comparisons between finite difference AMOS and Modified-Yee AMOS field calculations are provided.

Introduction

Cavity cells with geometrical complexity are usually modeled with staircased approximations to the surfaces. Depending on the level of the cell complexity, the task of gridding the device may be either impossible or unsatisfying. The well-known time domain discretization of Maxwell's equations (Finite-Difference Time-Domain FDTD), which was originally proposed by Yee [2], is the standard field solver currently employed. However, the algorithm's primary limitation for modeling curved surfaces lies in the fact that the fields are distributed on a logically regular grid system.

Holland [3] demonstrates that staircased approximations to oblique surfaces cause large errors for the scattering problems encountered in radar cross section calculations. The work of Craig and Anderson [4] shows that careful representation of localized features inside a cavity yields significant improvements over idealized models. Thus, it is often important to increase the geometrical accuracy of the model.

The Modified Finite Volume (MFV) algorithm proposed in [5] shows how electric and magnetic field components may be distributed on a nonorthogonal grid system. This type of field update scheme allows better boundary modeling. However, for the particular problem of the cavity cells, one needs a combination of the computationally efficient FDTD calculations in the interior with more accurate geometrical MFV type modeling on the simulation boundaries. Hence, in order to perform these hybrid calculations, we pursue a field solving scheme which is, in essence, the limiting case of MFV or a Modified-Yee procedure.

Numerical Procedure

The FD-AMOS wakefield code computes fields in the rotationally symmetric cavity. Hence, the fields are of the form

$$F = f_p \cos(n\phi) + f_q \sin(n\phi) \tag{1}$$

To perform the corresponding Modified-Yee calculation in $2 - 1/2$ D, placement of six field components on an irregular grid is required. Fig. 1 shows how the field components are distributed on a sample dual grid system. The nonorthogonal solid line mesh is the electric field grid, and the dashed line mesh is the magnetic field mesh.

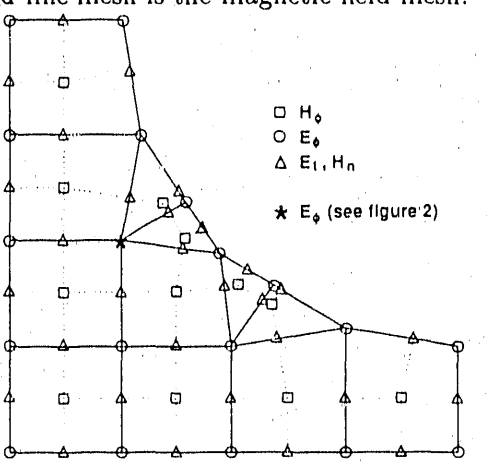

Fig. 1. Distribution of fields on sample irregular grid.

It can be readily seen that the two grids overlap in an orthogonal fashion. In cylindrical coordinates, E_ϕ nodes are distributed at intersections of solid lines and H_ϕ nodes are placed at intersections of dashed segments. The field components in the $r - z$ plane are located at the intersections of the two grids ($t \rightarrow$ 'tangential' and $n \rightarrow$ 'normal').

In order to describe the implications of this arrangement, we rewrite the EM time dependent curl equations

$$\nabla \times \vec{H} = \sigma \vec{E} + \epsilon \frac{\partial \vec{E}}{\partial t} + \vec{J}_s \tag{2}$$

$$\nabla \times \vec{E} = -\mu \frac{\partial \vec{H}}{\partial t} - \vec{K}_s \tag{3}$$

in the integral form

$$\oint \vec{H} \bullet d\vec{\ell} = \int\int \left(\sigma \vec{E} + \epsilon \frac{\partial \vec{E}}{\partial t} + \vec{J}_s\right) \bullet d\vec{A} \tag{4}$$

$$\oint \vec{E} \bullet d\vec{\ell} = -\int\int \left(\mu \frac{\partial \vec{H}}{\partial t} + \vec{K}_s\right) \bullet d\vec{A} \tag{5}$$

In Fig. 2, the graphical interpretation of Eqn. 4 - update of an E_ϕ node - is illustrated. This particular update

* Work performed under the auspices of the U. S. Department of Energy by LLNL under contract W-7405-ENG-48.

requires the values of the magnetic fields along the integration path with the contour integral being performed in the counterclockwise direction.

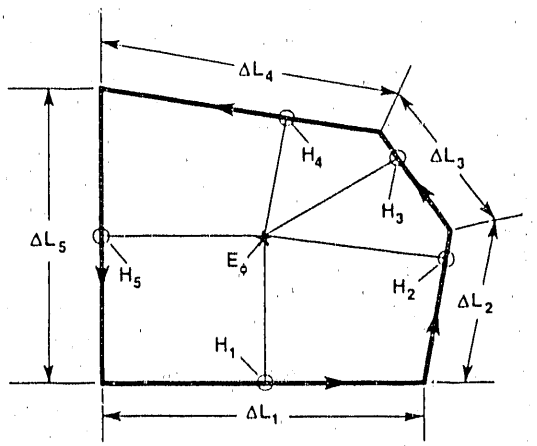

Fig. 2. Update diagram for E_ϕ node.

On the right hand side of Eqn. 4, the temporal derivative is performed by differencing the E_ϕ nodes at a time step k (previous time step) and $k+1$ (update time). The J conduction and source terms are assumed to be at the $k+1/2$ time step (current time). Hence, the explicit update equation for E_ϕ is given purely in terms of H fields and J_s. This update is precisely the same in both cylindrical and cartesian coordinates and may be written as

$$E_\phi^{k+1} = \frac{\frac{\{\sum_{i=1}^{m} H_i^{k+\frac{1}{2}}\ \Delta L_i\}}{A} - J_{s\phi}^{k+\frac{1}{2}} - E_\phi^k\{\frac{\sigma}{2} - \frac{\epsilon}{\Delta t}\}}{\left(\frac{\sigma}{2} + \frac{\epsilon}{\Delta t}\right)} \quad (6)$$

where A is the enclosed area, ϵ and σ are the permittivity and the conductivity, respectively, and Δt is the time increment.

To obtain the update equations for field components in the $r-z$ plane, the procedure is similar. However, the geometry of this case yields a contour path which requires integration of fields with a sinusoidal variation in ϕ. This ϕ dependence gives rise to a term with n as will be seen.

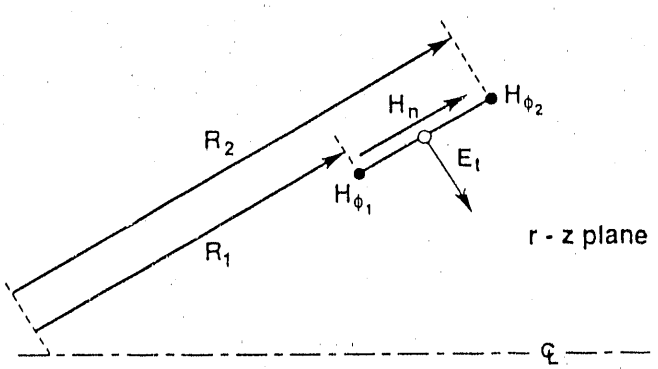

Fig. 3. Update for electric field node in the r-z plane.

For the general-oriented field component in the $r-z$ plane (Fig. 3), it can be seen that substituting Eqn. 1 into Eqn. 4 yields a discretized form given by

$$E_t^{k+1} = \frac{\frac{2.0\{r_2 H_{\phi_2}^{k+\frac{1}{2}} - r_1 H_{\phi_1}^{k+\frac{1}{2}} - n\ \Delta\ell H_n^{k+\frac{1}{2}}\}}{\{R_2^2 - R_1^2\}} - J_{st}^{k+\frac{1}{2}} - E_t^k\{\frac{\sigma}{2} - \frac{\epsilon}{\Delta t}\}}{\left(\frac{\sigma}{2} + \frac{\epsilon}{\Delta t}\right)} \quad (7)$$

where r_1 and r_2 are the radial distances to the H_{ϕ_1} and H_{ϕ_2} nodes, respectively, $\Delta\ell$ is the distance between ϕ nodes, and $R_2 > R_1$.

It should be noted that, if the field component is oriented with the field direction of positive slope (in $r-z$), the sign on n is switched to remain consistent with the convention of positive fields in the $+z$ direction. Next, we examine special cases involving E components which lie in the r and z direction. Referring to Fig. 3, one can see that as E_t becomes z-directed, $R_2 \rightarrow r_2$ and $R_1 \rightarrow r_1$. Hence, the update form for E_z follows immediately from Eqn. 7. The update of the E_r component is also similar in form to Eqn. 7. The primary difference is that the area enclosed by the integration path is $R\Delta\ell$, where R is the radial distance to the E_r node. Thus, one may write E_r as

$$E_r^{k+1} = \frac{\frac{\{R\ H_{\phi_2}^{k+\frac{1}{2}} - R\ H_{\phi_1}^{k+\frac{1}{2}} + n\ \Delta\ell\ H_n^{k+\frac{1}{2}}\}}{R\ \Delta\ell} - J_{sr}^{k+\frac{1}{2}} - E_\phi^k\{\frac{\sigma}{2} - \frac{\epsilon}{\Delta t}\}}{\left(\frac{\sigma}{2} + \frac{\epsilon}{\Delta t}\right)} \quad (8)$$

By duality, we obtain the discretized forms of the H field components which are

$$H_\phi^{k+1/2} = \frac{\frac{\{-\sum_{i=1}^{m} E_i^k\ \Delta L_i\}}{A} - K_{s\phi}^k + \frac{\mu}{\Delta t} H_\phi^{k-\frac{1}{2}}}{\frac{\mu}{\Delta t}} \quad (9)$$

$$H_n^{k+1/2} = \frac{\frac{2.0\{r_1 E_{\phi_1}^k - r_2 E_{\phi_2}^k + n\ \Delta\ell\ E_t^k\}}{\{R_2^2 - R_1^2\}} - K_{sn}^k + \frac{\mu}{\Delta t} H_n^{k-1/2}}{\frac{\mu}{\Delta t}} \quad (10)$$

$$H_r^{k+1/2} = \frac{\frac{\{R\ E_{\phi_1}^k - R\ E_{\phi_2}^k - n\ \Delta\ell\ E_t^k\}}{R\ \Delta\ell} - K_{sr}^k + \frac{\mu}{\Delta t} H_r^{k-1/2}}{\frac{\mu}{\Delta t}} \quad (11)$$

The principal reason for this approach in discretization is that one may easily match a FDTD grid to the nonorthogonal body fitting grid. In Fig. 1, the edges of the irregular piece fit exactly into an FD grid. As mentioned previously the irregular grid calculations require a large amount of information storage per node, primarily involving the spatial interelationships between nodes. If

there are large interior free space regions, as in cavities, calculations are more efficiently performed on finite difference cells where spatial relationships between nodes are implicit, and thus, from a computational point of view, do not need to be stored.

Propagation Results

In this section we perform a calculation to illustrate the notion of mixed FDTD and irregular mesh calculations. Referring to Fig. 4, we perform a numerical propagation experiment involving a coaxial structure.

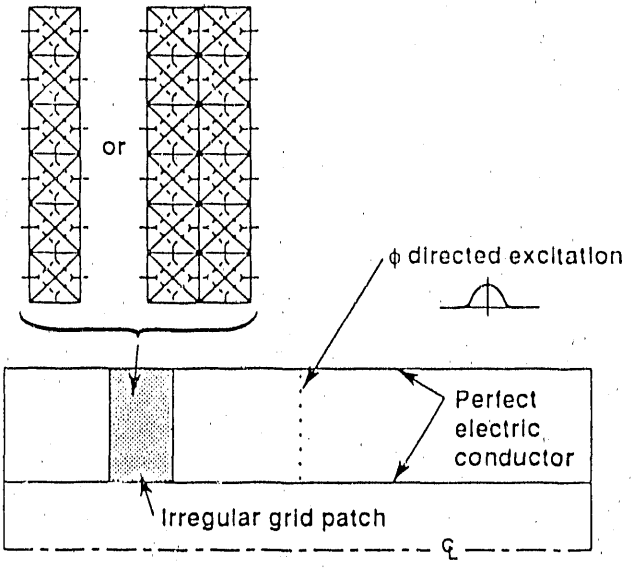

Fig. 4. Propagation in a coaxial structure.

A gaussian pulse with a $1/r$ dependence is driven in the center of the coax (in z). On the left hand side, we insert irregular grid patches that match exactly into the finite difference cells. At $t = 0$, we drive the nodes with a ϕ-directed excitation. Two identical TEM pulses are formed, with one traveling to right and the other to the left. It is found that the pulse, which must propagate through the irregular patch, emerged on the left of the patch with minimal reflection (Fig. 5).

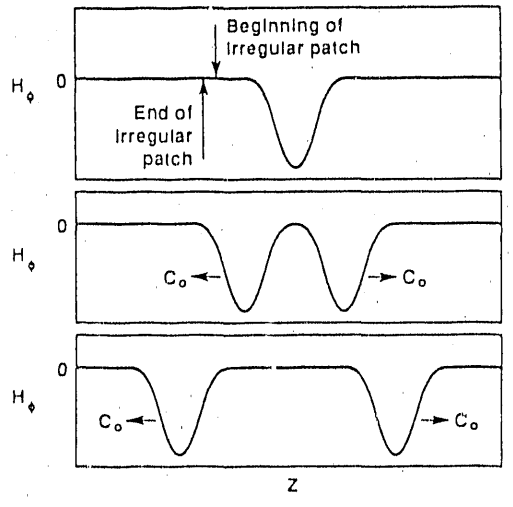

Fig. 5. Propagation of the TEM pulse through the irregular patch.

An effective reflection coefficient is computed by calculating the energy contained in the pulse after it emerges from the irregular patch (E_a) and then comparing it to the energy contained in the pulse just prior (E_b) to entering the irregular region, i.e.,

$$R_{eff} = \{1 - \frac{E_a}{E_b}\}. \tag{12}$$

The effective reflection coefficient (energy) for the patch of single cell thickness was found to be 3.280e-4. Calculations involving thicker irregular patches such as the two cell wide supergrid (Fig. 4) were performed, resulting in accuracies similar to those observed in the first case. The effective reflection coefficient for the two cell wide supergrid was approximately 5.303e-4.

When modeling curvilinear or oblique surfaces (in $r-z$), one would not, in most instances, use irregular patches much more than two cells thick. The results from the numerical propagation tests seem to indicate that, at these patch thicknesses, the small numerical reflections may be to some extent typical. However, there could be instances where an irregular mesh of poor quality (i.e., nodes poorly distributed) might lead to problems in numerical reflections, phase velocity, and/or stability. We are investigating the effectiveness of the procedure in the different regimes in order to gauge the robustness of the algorithm.

Conclusions

We have demonstrated a field solver on an irregular dual grid system which will match into FD cells. The orthogonality between the overlapping dual grids permits simultaneous FD and irregular Modified-Yee calculations. This is useful since we may now model simulation boundaries with a greater degree of accuracy, and simultaneously, in regions away from the boundaries, update fields which remain distributed on finite difference cells.

References

1. J. F. DeFord, G. D. Craig, and R. R. McLeod, "The AMOS Wakefield Code," in *Proceedings of the Conference on Computer Codes and the Linear Accelerator Community*, Los Alamos, New Mexico, Jan. 22-25, 1990, pages 265-289.
2. K. S Yee, "Numerical Solution of Initial Boundary Value Problems Involving Maxwell's Equations in Isotropic Media," *IEEE Transactions on Antennas and Propagation*. Volume AP-14, May 1966, pages 302-307.
3. R. Holland, "The Case Against Staircasing," *Proceedings of the Sixth Annual Review of Progress in Applied Computational Electromagnetics*," 19-22 March 1990, pages 89-95.
4. G. D. Craig and B. Anderson, private communication, January 1990.
5. N. K. Madsen and R. W. Ziolkowski, "Numerical Solution of Maxwell's Equations in the Time Domain Using Irregular Nonorthogonal Grids," Wave Motion 10 (1988), pages 583-596.

END

DATE FILMED

10 / 17 / 90